Climate Dynamics (2000) 16:491–500

L. D. D. Harvey

An assessment of the potential impact of a downward shift of tropospheric water vapor on climate sensitivity

Received: 23 February 1998 / Accepted: 1 November 1999

Abstract This work uses an energy balance climate model (EBCM) with explicit infrared radiative transfer, parametrized tropospheric temperature and humidity profiles, and separate stratosphere, troposphere, and surface energy balances, to investigate claims that a downward redistribution of tropospheric water vapor in response to surface warming could serve as a strong negative feedback on climatic change. A series of sensitivity tests is carried out using: (1) a variety of relationships between total precipitable water in the troposphere and temperature; (2) feedbacks between surface temperature and the vertical distribution of tropospheric water vapor at low latitudes; and (3) feedback between surface temperature or meridional temperature gradient and lapse rate. Fixed relative humidity (RH) enhances the global mean surface temperature response to a CO_2 doubling by only 50% compared to fixed absolute humidity, giving a response of 1.8 K. When water vapor is assumed to be redistributed downward between 30°S–30°N such that a 1 K surface warming reduces total precipitable water above 600 hPa by 10%, the global mean surface air temperature response is reduced to 1.2 K. Assuming a stronger downward redistribution in relation to surface temperature change has a rapidly diminishing marginal effect on global mean and tropical surface temperature response, while slightly increasing the warming at high latitudes due to the parametrized dependence of middle-to-high latitude lapse rate on the meridional temperature gradient. A modest downward water vapor redistribution, such that absolute humidity in the upper troposphere at subtropical latitudes is constant as total precipitable water increases, can reduce the tropical temperature sensitivity to less than 1 K, while increasing the equator-to-pole amplification of the surface air temperature response from a factor of about three to a factor of four. However, it is concluded that whatever changes in future GCM response might occur as a result of new parametrizations of subgrid-scale processes, they are exceedingly unlikely to produce a climate sensitivity to a CO_2 doubling of less than 1 K even if there is a strong downward shift in the water vapor distribution as climate warms.

L. D. D. Harvey
Department of Geography, University of Toronto,
100 St. George Street, Toronto, Canada M5S 3G3

1 Introduction

In three dimensional atmospheric general circulation models (GCMs), as well as in one dimensional radiative convective models (RCMs) with fixed relative humidity (RH), the increase in atmospheric water vapor content that accompanies overall warming following a CO_2 increase constitutes the single most important positive feedback. In a pioneering study using an RCM, Manabe and Wetherald (1967) found that the assumption of fixed RH amplified the surface temperature warming following a CO_2 increase by a factor of 1.77 compared to the case with fixed absolute humidity. In GCMs, RH is a freely predicted quantity, but tends to be approximately constant as the model climate changes. Hansen et al. (1984) find that, for the steady state following a CO_2 doubling, the atmospheric water vapor content increases by 33% in their GCM and, further, that this increase alone increases the global mean surface-troposphere heating by about 6 W m^{-2}. This is about 50% larger than the initial, direct heating of 4 W m^{-2} caused by the CO_2 doubling, and therefore more than doubles the climatic response compared to fixed absolute humidity. The climatic response in their model is further amplified by an upward shift in the water vapor distribution as climate warms, which leads to an additional heating of 3 W m^{-2}. Manabe and Wetherald (1980) report a reduction in the upward infrared flux at the top-of-the-atmosphere for a CO_2 quadrupling of 4.26 W m^{-2}, with a further reduction of 6.68 W m^{-2} due to the steady state water vapor change. In a later version of the same model, infrared reductions of 3.2 W m^{-2} and 6.2 W m^{-2} due to CO_2 and water vapor changes, respectively, are reported (Spelman and Manabe 1984).

The viewpoint that increases in water vapor constitute a strong positive feedback has been challenged by Lindzen (1990). He argues that increased cloud convection due to overall warming will lead to a drying of the upper troposphere through the increase in subsidence between clouds which would be induced. Since increased convection also implies increased upward moisture transport within cumulus towers, some of which will detrain and evaporate rather than falling out as rain, the net effect on upper tropospheric moisture will depend in part on how the precipitation efficiency changes. This refers to the fraction of upward moisture transfer that immediately falls as precipitation. If, as the degree of upward moisture pumping increases, a smaller fraction goes into moistening the upper troposphere and more into immediate precipitation, then the net effect could be a drying of the upper troposphere. Calculations by Sun and Lindzen (1993; their Fig. 20) indicate that the time required for raindrops to form decreases as temperature increases, which implies that the precipitation efficiency should increase.

Since, molecule-per-molecule, water vapor in the upper troposphere is more effective in trapping heat than in the lower troposphere, a downward redistribution of water vapour constitutes a negative feedback. However, total column water vapor amount clearly increases as sea surface temperature increases; the relationship in the tropics is weak at the monthly and annual time scales, where concurrent changes in atmospheric dynamics complicate the picture, but is stronger at the decadal time scale (Gaffen et al. 1992). The net effect on climatic sensitivity would then depend on the effect of changes in both total column water vapor amount and its vertical distribution. Furthermore, there is no reason to expect that drying of the upper troposphere would occur outside the tropics as the climate warms, since eddies and mean meridional motions are the dominant factors influencing upper tropospheric moisture outside the tropics, and their moistening effect would increase as the climate warms (del Genio et al. 1994).

Lindzen's (1990) hypothesis sparked a number of observationally based and theoretical studies assessing the relationship between convection and upper tropospheric water vapor. Direct observations of the relationship between the intensity of convection and atmospheric moisture variations between different seasons and different regions have been interpreted as implying that increasing convection moistens the entire troposphere (Rind et al. 1991; Inamdar and Ramanathan 1994). However, this correlation could be due in part to differences in atmospheric dynamics (i.e., a shift from lower level convergence to divergence) between the regions and seasons with weak and strong convection. Sun and Oort (1995) attempted to circumvent this problem by examining the correlation between atmospheric water vapor and surface temperature averaged over the entire tropics (30°S–30°N). Based on radiosonde data for the period May 1963 to December 1989, they found that the amount of water vapor in the tropical atmosphere increased with increasing temperature as follows:

1. By 70–75% of the increase that would occur with fixed RH in the 1000–900 hPa layer
2. By only 15% of the increase expected with fixed RH at 700 hPa
3. By 70% of the increase expected with fixed RH at 300 hPa

In the planetary boundary layer (1000–900 hPa), the change in water vapor is most directly tied to the thermodynamically driven increase in the rate of evaporation. There is also a sizeable relative increase in the upper troposphere, related, no doubt, to an increase in the rate of detrainment of moisture from the tops of cumulus cloud columns. However, in the middle troposphere there is almost no increase in the amount of water vapor, which can be explained by an increase in the rate of subsidence of relatively dry air from the upper troposphere, in line with Lindzen's (1990) argument. Simulations with the GISS GCM (del Genio et al. 1991) and the UKMO GCM (Mitchell and Ingram 1992) using convective cloud schemes that account for subsidence between clouds indicate that increasing convection moistens the upper troposphere, although the two models disagree as to the magnitude of the moistening: in the case of the GISS GCM, RH is constant near the surface but increases in the global mean by an amount which grows with increasing height to 5% of saturation at the 200 hPa level, whereas in the UKMO GCM, the global mean RH decreases by an average of about 2–3% of saturation between 550–250 hPa. The latter corresponds to absolute humidity increasing by about 50% of the increase that would occur with constant RH.

Soden (1997) examined the relationship between clear-sky greenhouse trapping (GHT) and sea surface temperature in observed data, where GHT is simply the difference between the surface emission (σT^4) and the outgoing emission for clear skies at the top-of-the-atmosphere. For the period April 1985 to December 1987, he found that the tropical-mean GHT increased in association with an increase in tropical-mean SST, as conditions changed from La Niña to El Niño. GHT trapping increased in regions where deep convection increased, and decreased elsewhere (due to an increase in subsidence). There were marked intra-annual variation in GHT that are not reflected in changes in the tropical-mean SST. This must be related to changes in the spatial patterns of SST, which are known to be as important to the occurrence of deep convection as absolute temperatures (Zhang 1993). Since it is not clear how the spatial patterns of SST will change as the climate warms or whether the patterns of temperature change will resemble El Niño patterns, the correlation seen over the course of a La Nina–EL Niño transition might not apply to a warmer climate. However, the GFDL atmospheric general circulation model (AGCM) has successfully simulated the overall variation in tropical-mean GHT from 1985–1989, in tropical-mean intra-annual fluctua-

tions, and the local patterns of increasing and decreasing GHT when forced with observed changes in SST. This model, like all AGCMs, produces a positive longterm water vapor feedback. This test suggests that, *given the correct patterns of sea surface temperature change*, current AGCMs should do a reasonable job in simulating the water vapor feedback in tropical regions.

Sinha and Allen (1994) examined the effect of convection and convection-induced subsidence, in isolation, and concluded that an increase in the intensity of convection can cause the upper troposphere to become dryer in some height intervals, depending on the choice of model parameters which are themselves highly uncertain. For two intermediate cases they obtained peak drying by 10% centered at heights of 500 hPa and 250 hPa in response to a 1 K surface warming, with less drying at other heights in the upper troposphere and moistening close to that expected for constant RH below a height of 700 hPa. The model used by Sinha and Allen (1994) adopts one of the key assumptions of Lindzen's (1990) original hypothesis, that all condensed water vapor in deep clouds falls to the ground as rain rather than partially evaporating and moistening the upper troposphere, an assumption that had been refuted by subsequent model-based analysis of observations (Sun and Lindzen 1993). Relaxation of this assumption may very well cause the simulated upper troposphere drying to disappear. del Genio et al. (1991) allowed for detrainment of ice crystals from cumulus cloud tops in their simulation, which undoubtedly contributed to the upper level moistening found in their simulation. Sinha and Allen (1994) indicate that introduction of other processes can also substantially reduce the drying, but that introducing yet further processes can bring it back.

Shine and Sinha (1991) examined the effectiveness of changes in the amount of water vapor in changing the Earth's climate as a function of the height interval where the water vapor change occurs. They found that, although a given absolute change in water vapor amount is much more effective above 400 hPa in changing the Earth's climate, the climate is more sensitive to a given relative change in the lower troposphere than in the upper troposphere. However, it is not clear from this study what the net effect on the radiative balance would be of a downward redistribution of water vapor. Furthermore, any negative feedback arising from a downward shift in water vapor would be restricted to those low-latitude regions where convection-induced subsidence dominates the vertical water vapor distribution.

The purpose of this study is to assess the effect on zonal mean and global mean climate sensitivity of a hypothetical downward redistribution of water vapor in low-latitude regions as climate warms and as the total column precipitable water vapor amount increases. A downward redistribution of water vapor from above the 600 hPa level to below the 600 hPa level is imposed in the 30°S–30°N latitude band, while allowing water vapor to increase at all heights outside these regions. Although the bulk of the evidence does not support Lindzen's (1990) hypothesis of a negative water vapor feedback, it is important, given the potential implications to human societies and natural ecosystems of climatic warming of the magnitude projected by current models, to examine hypotheses which challenge the conventional viewpoint in as many different ways as possible.

This work does not attempt to simulate the quantitative change in water vapor distribution and other parameters accompanying global warming based on first principles, since it is unclear whether even GCMs are capable of providing quantitatively accurate results (as noted, different GCMs give different vertical profiles of RH change). Rather, this work is intended as a sensitivity study. The important constraints are to allow for a latitudinal variation in the hypothesized feedback processes in assessing the global mean climate response, and to perform accurate radiative transfer calculations. For these reasons, the latitudinally resolved energy balance climate model (EBCM) of Harvey (1988a,b) is utilized, with the original parametrized infrared emission replaced with explicit radiative transfer calculations. To do this requires specifying the vertical profiles of temperature, water vapor, and other radiatively active gases, as well as specifying the vertical position of cloud. This framework allows one to explicitly prescribe various hypothetical or observationally based changes in the water vapor profile as surface temperature changes, and to determine the interactive effect of these changes, along with model surface albedo feedbacks, on the climatic response.

Radiative feedbacks have been studied in the past using RCMs, but there would be no advantage to embedding an RCM in the EBCM used here. This is because, in RCMs, the critical lapse rate for convective mixing, the vertical profile of RH, and their variation (if any) with climate have to be prescribed, yet these prescribed parameters largely determine the model sensitivity (Chylek and Kiehl 1981; Hummel and Kuhn 1981). Specifying the initial temperature and RH profiles, and their variation as climate changes, as is done here, is equivalent to what is done in RCMs. However, the use of an EBCM allows for latitudinal variation in the prescribed lapse rate feedback. Furthermore, as discussed by Stone and Charlson (1979), there are theoretical reasons for expecting that the temperature lapse rate in mid-to-high latitudes depends on the meridional temperature gradient, something that would be affected if there is a negative water vapor feedback operating in low-latitude regions only. Hence, there is a potential interaction between low-latitude water vapor feedback and middle-to-high latitude lapse rate feedback, an interaction which is best explored using the relatively simple model that is presented here.

2 Model description and parametrized feedbacks

The EBCM used for this study (Harvey 1988a) has latitudinal, surface-air, and land-sea resolution. The oceanic part of each lat-

itudinal zone contains an isothermal mixed layer which varies in depth from 75 m at the equator to 125 m at the poles. Meridional sensible heat transport occurs in the mixed layer and atmosphere by linear diffusion; as well, linear diffusion of latent heat occurs in the atmosphere poleward of 20° based on the meridional gradient of atmospheric vapor pressure. The distinction between sensible and latent heat allows the meridional heat flux in mid-to-high latitudes to remain approximately constant as the climate warms, in spite of a decrease in the meridional temperature gradient, in agreement with GCMs (Wetherald and Manabe 1975). Radically different formulations of the meridional heat transport, such as making the low latitude transport depend in part on absolute vapor pressure, do not change the key conclusions arising from this study. Thus, the use of diffusion to link temperature perturbations at different latitudes is sufficient for the purposes of this work. Absorption of solar radiation by the atmosphere and surface is computed using the parametrizations of Lacis and Hansen (1974). In the original model, the infrared emission to space is computed using the parametrization of Thompson and Warren (1982).

For this study, the parametrized infrared fluxes are replaced with explicit radiative transfer calculations using the infrared subroutines from the NCAR Community Climate Model, Version 2. This package uses the nonisothermal emissivity and absorptivity parametrization for water vapor of Ramanathan and Downey (1986), the 15 μm CO_2 absorptance parametrization of Kiehl and Briegleb (1991), and the 9.6 μm O_3 absorptance parametrization of Ramanathan and Dickinson (1979). The water vapor parametrization includes the effects of the continuum absorption.

The original model does not distinguish between the troposphere and stratosphere, but this distinction is required here since the surface-troposphere system warms together in response to a CO_2 increase, while the stratosphere cools, and about 40% of the global mean surface-troposphere heating due to a CO_2 increase is a result of increased downward infrared emission from the stratosphere. Separate stratosphere and troposphere energy balances are computed for the present study, from which mean stratospheric and surface air temperatures are computed. A globally uniform stratospheric thickness of 200 hPa is assumed, and a single, zonally averaged stratospheric temperature is computed based on the absorption of solar energy and net emission of infrared radiation by the stratosphere and a latitudinally and seasonally varying dynamical heating term. Monthly values of the dynamical heating term Q_{dyn} were computed from the equation

$$R\frac{\mathrm{d}T_{st}}{\mathrm{d}t} = Q_{dyn} + Q^* \tag{1}$$

where R is the stratospheric thermal inertia (J m^{-2} K^{-1}), T_{st} is the observed, zonally averaged, monthly mean temperature at 100 hPa, and Q^* is the model-computed stratospheric net radiation. Observed stratospheric, surface, and surface air temperatures (combined with the model-parametrized tropospheric lapse rate and RH profiles) were used to compute Q^*. Global mean values of Q^* were on the order of a few W m^{-2}, so Q^* was adjusted to give a global mean of zero for each month. This is consistent with the finding of Ramanathan and Dickinson (1979) and others that the stratosphere is in approximate radiative balance.

Explicit infrared radiative transfer computation requires specification of the humidity and temperature profiles through the atmosphere. The variation of RH with height in the troposphere for the spinup is computed using the formulation of Ramanathan and Coakley (1978) with observed temperatures as input. For temperature, I have slightly modified the approach proposed by Stone and Carlson (1979), in which the lapse rate is set to the smaller of the moist adiabatic lapse rate, γ_m, and the critical lapse rate for baroclinic instability, γ_c. The critical lapse rate is given by

$$\gamma_c = \gamma_d + \beta\frac{\tan\phi}{H}\frac{\partial T}{\partial\phi} \tag{2}$$

where γ_d is the dry adiabatic lapse rate and H is the scale height. The original parametrization is based on the meridional temperature gradient at the mid troposphere level. Here, I use the meridional gradient of surface air temperature as this is the only tropospheric temperature which is prognostically determined by the model, and introduce the factor β, which is tuned so as to give approximately the same γ_c values as reported by Stone and Carlson (1979) when observed surface air temperatures are used as the input. The resulting values vary piecewise linearly in both hemispheres from 0.9 at 45° latitude, to 0.65 at 60° latitude, to 0.30 at 75° latitude, to 0.0 at the poles. Although the observed lapse rate is close to γ_m at low latitudes, there are significant departures in the lower tropical atmosphere. We therefore compare γ_c with the tropospheric mean of a modified moist adiabatic lapse rate, γ_m^*, which is given by

$$\gamma_m^* = \alpha_1\gamma_d + (1-\alpha_1)\gamma_m \tag{3}$$

where

$$\alpha_l = \begin{cases} w(\phi)\left(1-\left(\frac{P_s-P}{300}\right)^{0.25}\right) & P > 700 \\ 0 & P \le 700 \end{cases} \tag{4}$$

and $w(\phi)$ is 1.0 between 0–20° latitude, 0.0 poleward of 35° latitude, and varies linearly with latitude in between. According to Eqs. (3) and (4), $\gamma_m^* = \gamma_m$ above 700 hPa and poleward of 35°, but approaches γ_d near the surface at low latitudes. This gives a rough fit to data reported by Stone and Carlson (1979) equatorward of about 40°. At each latitude the model lapse rate is set to the smaller of γ_m^* and γ_c (γ_m^* is smaller than γ_c equatorward of about 30° for the present climate).

For all experiments reported here, eight tropospheric layers of 100 hPa thickness each are used for radiative transfer calculations, as doubling the resolution has negligible effect on fluxes and flux sensitivity. Separate infrared and solar fluxes are computed for clear and cloudy sky cases and weighted according to the observed zonally averaged, monthly cloud fractions for land and sea. Most of the feedbacks considered here have very different strengths for clear and cloudy sky cases, so the specified cloud fractions are important to the climatic sensitivity. The global mean cloud fraction for the dataset used here is 0.61, which falls in the middle of the range of 0.61 ± 0.01 reported by Mokhov and Schlesinger (1994) for surface-based analysis and near the high side of the range of 0.57 ± 0.05 obtained by various satellite-based analyses. For the cloudy sky case, a single cloud layer is used, with cloud-top pressures chosen so as to give close to the observed mean annual infrared emission to space when observed surface and surface air temperatures are used. This tuning produces cloud top heights which vary smoothly from 800 hPa at the North Pole at 400 hPa at the equator to 600 hPa over Antarctica. Figure 1 compares the model computed and observed latitudinal variation of zonal mean infrared emission to space using observed temperatures, as well as observed and model computed mean annual surface air temperatures. As can be seen from Fig. 1, the model performs well. The model-simulated seasonal variation in hemisphere sea ice and land snow area also compares well with observations.

3 Perturbation experiments

The model is perturbed by a sudden doubling of atmospheric CO_2 concentration, and a new steady state climate is computed. The following options are tested with regard to lapse rate and atmospheric humidity:

3.1 Tropospheric humidity

We consider six cases with regard to column water vapor in the perturbation runs: (1) fixed absolute humidity; (2) absolute humidities at all heights over land and ocean at a given latitude scaled by the relative increase in ocean surface vapor pressure at the given latitude; (3) fixed RH; (4) RH increasing as climate warms; (5) fixed RH followed by a downward redistribution of water vapor such that the precipitable water W above the 600 hPa level is reduced by a given percentage of the initial amount for latitudes between 30°S–

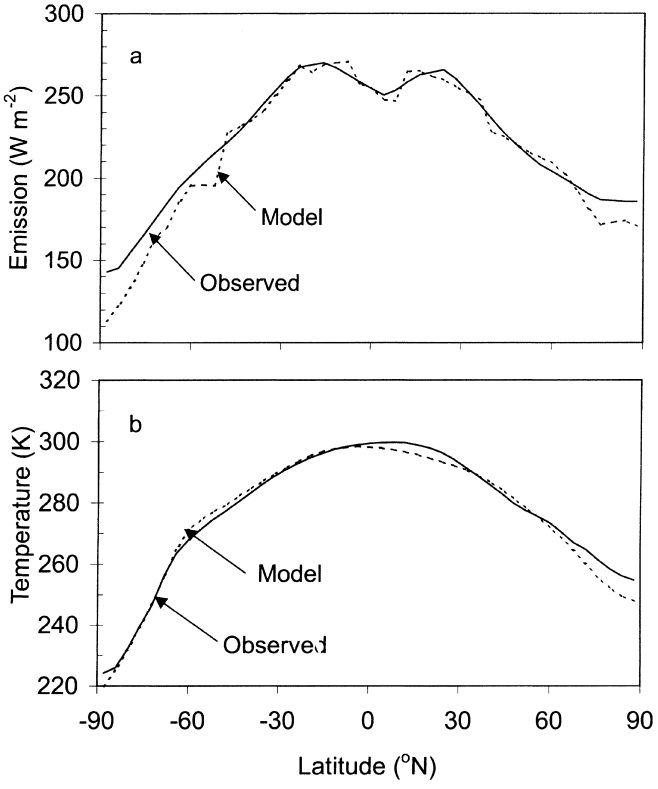

Fig. 1 a Comparison of observed zonally averaged, mean annual infrared emission to space and that computed by the model using observed surface and surface air temperatures as input. **b** Comparison of observed and model predicted latitudinal variation of zonally averaged, mean annual surface air temperature

30°N, where Lindzen's (1990) hypothetical cumulus drying effect might be dominant; and (6) absolute humidity scaled as in (2) and then shifted as in (5). For the fixed-RH case the percentage increase in absolute humidity increases with increasing height; scaling all humidities by the increase in ocean surface vapor pressure therefore results in a decrease in RH which grows with increasing height as climate warms, and produces a change in total precipitable water which is similar to that found by Sun and Oort (1995) in the tropics at the interannual time scale. The increasing RH case is implemented using the formula

$$RH(\Delta T_s, P) = RH(0, P) + \alpha_2 \Delta T_s \left(\frac{P_0 - P}{800}\right) \tag{5}$$

where $\alpha_2 = 0.0125$. Using Eq. (5), a 4 K surface warming results in no increase in RH near the surface and a 5% increase at the 200 hPa level, which roughly matches the changes obtained by del Genio et al. (1991) for the GISS GCM. For cases (5) and (6), the initial total precipitable water vapor amount $W(0)$ above 600 hPa between 30°N–30°S is adjusted as,

$$W(\Delta T_s) = W(0)(1 + \alpha_3 \Delta T_s) \tag{6}$$

and the excess moisture relative to the fixed RH or scaled humidity case is uniformly distributed between 600 hPa and the surface. In most cases, $\alpha_3 = -0.1$, so that a 1 K warming produces a 10% decrease in precipitable water vapor above 600 hPa, as suggested by the results of Sinha and Allen (1994). Constant RH or scaled humidity is assumed outside the 30°S–30°N region for this case.

3.2 Lapse Rate

Tropospheric lapse rates are either frozen at the seasonally and latitudinally varying values obtained at the end of the spinup run or continue to be parametrized as in the spinup run. In either case, stratospheric temperature responds freely to the CO_2 perturbation. As in previous work with RCMs, there is not guarantee that the changes in lapse rate are consistent with the prescribed changes in RH profile. However, given that the sole purpose of this exercise is to determine how small we can possibly reduce the climate sensitivity, this is not of concern here.

4 Results

4.1 Infrared flux sensitivity

The steady state global mean surface temperature response ΔT_s to a heating perturbation ΔQ can be written as

$$\Delta T_s = \frac{\Delta Q}{\lambda} \tag{7}$$

where

$$\lambda = \frac{\mathrm{d}F}{\mathrm{d}T_s} - \frac{\mathrm{d}S}{\mathrm{d}T_s} \tag{8}$$

is the radiative damping parameter, F is the net upward infrared flux at the tropopause (equal to the upward flux minus the downward flux), and S is the solar flux absorbed by the surface-troposphere system. The appropriate ΔQ to use is the perturbation in net radiation at the tropopause, after allowing for the adjustment of stratospheric temperatures (see Chapter 3 of Harvey 2000). The infrared flux sensitivity $\mathrm{d}F/\mathrm{d}T_s$ can be decomposed as

$$\frac{\mathrm{d}F}{\mathrm{d}T} = \frac{\partial F}{\partial T} + \sum \frac{\partial F}{\partial I}\frac{\mathrm{d}I}{\mathrm{d}T} \tag{9}$$

where the summation is over all internal variables I. For the particular case of fixed RH and variable lapse rate, with all other variables held constant,

$$\frac{\mathrm{d}F}{\mathrm{d}T_s}|_{RH} = \frac{\partial F}{\partial T} + \frac{\partial F}{\partial wv}\frac{\partial wv}{\partial T_s}|_{RH,\gamma} + \frac{\partial F}{\partial wv}\frac{\partial wv}{\partial \gamma}\frac{\mathrm{d}\gamma}{\mathrm{d}T_s} + \frac{\partial F}{\partial \gamma}\frac{\mathrm{d}\gamma}{\mathrm{d}T_s} \tag{10}$$

The first term on the right hand side arises from the dependence of infrared emission on temperature through the Planck function. The second term is a pure water vapor feedback, while the fourth term is a pure lapse rate feedback. The third term is a mixed water vapor-lapse rate feedback. Since the lapse rate tends to decrease with increasing surface temperature in the moist tropical regions, the temperature increase in the middle and upper troposphere is larger than for fixed lapse rate. Assuming fixed RH, this gives a larger water vapor increase (and stronger water vapor feedback) than if lapse rate were constant.

Here, $\partial F/\partial T$ is computed by comparing the net flux at the tropopause before and after imposing a 1 K warming of the surface and troposphere with all other variables held constant. The pure water vapor feedback is computed by imposing a uniform 1 K warming, recomputing water vapor amounts assuming constant RH,

determining dF/dT by comparing fluxes before and after the perturbation, and subtracting the previously determined $\partial F/\partial T$. From Eqs. (7) and (8), the climate sensitivity is multiplied by a factor of $(\partial F/\partial T)/(\partial F/\partial T + \partial F/\partial(\mathrm{wv})\partial(\mathrm{wv})/\partial T)$ due to the water vapor feedback in the infrared part of the spectrum. A similar analysis is applicable to the solar part of the spectrum.

As summarized by MacKay and Khalil (1991), previous workers have calculated that the water vapor feedback enhances climate sensitivity by 55% to 77% if fixed RH is assumed, depending on the radiation code used and the assumed cloudiness and cloud heights. As a point of reference in analyzing the model response obtained here, I have calculated $\partial F/\partial T$ and $\partial F/\partial(\mathrm{wv})\partial(\mathrm{wv})/\partial T$ assuming fixed RH for clear and cloudy skies for the standard Tropical, Mid-Latitude Summer, Mid-Latitude Winter, and Polar atmospheric profiles of McClatchey et al. (1971). Results are given in Table 1, along with the enhancement in climate sensitivity based on clear sky and cloudy sky feedbacks alone. The clear sky enhancement due to water vapour feedback with fixed RH ranges from 23% (Polar) to 86% (Tropical), while the cloudy sky enhancement ranges from 24% (Polar) to 57% (Tropical). The clear sky enhancement is largest for the warm tropical profile because saturation vapor pressure increases most rapidly with increasing temperature at high temperatures. The difference between the global mean water vapor feedback obtained here (about 50%) and that obtained by other workers with fixed RH (55–77%), represents the effect of the third term in Eq. (10). This water vapor-lapse rate interaction term is of particular importance in the case of the NCAR AGCM, in as much as Zhang et al. (1994) deduced that the total water vapor feedback was sufficient to increase the climate sensitivity by 107% based on clear sky regions, and by 91% based on the cloudy sky regions, in spite of the fact that RH decreases through much of the atmosphere in their simulation.

Table 2 shows global and annual mean clear-sky and cloudy-sky dF/dT_s and dS/dT_s values for the experiments performed here with the climate model. Also given is the net global radiative damping, λ. Assuming fixed RH reduces the mean-sky dF/dT by 24%. Allowing RH to increase by 5% at the 200 hPa level per degree surface warming, as in the GISS GCM, reduces the mean sky dF/dT_s by a further 21%. Initially assuming fixed RH, then shifting precipitable water downward such that the amount of water above 600 hPa decreases

Table 1 Infrared flux sensitivites at the tropopause for the Tropical, Mid-Latitude Summer, Mid-Latitude Winter, and Polar profiles of McClathey et al. (1971). $\partial F/\partial T$ is the flux sensitivity when temperature alone changes, while $\partial F/\partial(\mathrm{wv})/\partial(\mathrm{wv})/\partial T$ is the contribution to dF/dT from changes in water vapor under the assumption of fixed RH and lapse rate. The last two columns give the clear (cloudy) sky enhancement of climate sensitivity that would occur if the clear (cloudy) sky feedback strength were to operate for all skies. ML, Mid-Latitude

Case	$\partial F/\partial T$		$\partial F/\partial(\mathrm{wv})\partial(\mathrm{wv})/\partial T$		dF/dT		Enhancement	
	Clear	Cloudy	Clear	Cloudy	Clear	Cloudy	Clear	Cloudy
Tropical	4.49	4.30	−2.07	−1.56	2.42	2.74	86%	57%
ML Summer	4.27	4.14	−1.67	−1.37	2.60	2.77	61%	49%
ML Winter	3.57	3.48	−0.91	−0.77	2.66	2.71	34%	28%
Polar	3.14	3.17	−0.58	−0.61	2.56	2.55	23%	24%

Table 2 Infrared, solar, and total radiative damping for various experiments, global mean equilibrium temperature change as obtained by the climate model, equatorial warming, and the ratio of polar to equatorial warming

Case	dF/dT		$-dS/dT$		Total global			
	Clear	Cloudy	Clear	Cloudy	λ	ΔT	ΔT_{tr}	Amp
With fixed lapse rate								
Fixed e_a	3.95	3.43	0.01	0.01	3.54	1.00	0.77	2.2
Fixed RH	2.53	2.96	−0.24	−0.19	2.44	1.50	1.11	2.4
Increasing RH	1.46	2.40	−0.32	−0.15	1.60	2.36	1.45	2.6
Fixed + Shifted RH	3.36	3.37	−0.16	−0.17	3.15	1.13	0.93	2.3
With variable lapse rate								
Fixed e_a	4.10	3.91	0.01	0.01	3.78	0.94	0.60	4.0
Fixed RH	2.60	3.86	−0.31	−0.22	2.82	1.28	0.98	2.8
Increasing RH	1.61	3.40	−0.39	−0.21	2.08	1.79	1.17	3.2
Fixed + Shifted RH	3.45	3.88	−0.18	−0.28	3.28	1.09	0.64	4.6
With scaled e_a and variable lapse rate								
No shift	3.41	3.74	−0.13	−0.25	3.26	1.09	0.71	3.9
$\alpha = -0.0$	3.50	3.74	−0.09	−0.27	3.35	1.08	0.67	4.2
$\alpha = -0.1$	3.63	3.68	−0.09	−0.27	3.35	1.06	0.60	4.8
$\alpha = -0.3$	3.87	3.60	−0.04	−0.29	3.42	1.03	0.50	6.2
$\alpha = -0.5$	4.11	3.56	−0.00	−0.30	3.53	1.00	0.41	7.5

by 10% for each degree surface warming, increases dF/dT_s by 23% (fixed lapse rate) or 11% (variable lapse rate) compared to the corresponding fixed RH case.

Figure 2 shows the latitudinal variation of dF/dT_s for selected cases. dF/dT_s is fairly uniform with latitude for the case with fixed RH or absolute humidity and fixed lapse rate. Introduction of variable lapse rate (Fig. 2a) increases dF/dT by 1–2 W m^{-2} K^{-1} at low latitudes (where lapse rate decreases) and decreases it by up to 1.5 W m^{-2} K^{-1} at high latitudes (where lapse rate increases), such that global mean dF/dT increases (Table 2). When water vapor is shifted downward as T_s increases, dF/dT_s increases by 1–2 W m^{-2} K^{-1} in the regions where the downward shift occurs (Fig. 2b).

Further insight into the radiative impact of water vapor feedbacks can be obtained by imposing various changes in the water vapor amount and profile with fixed temperatures. Table 3 shows the impact on net upward infrared flux at the tropopause for the tropical profile of McClatchey et al. (1971) when total precipitable water is increased by 10%, 20%, or 30% with either no change in the shape of the humidity profile, no increase above 600 hPa, or decreases of 10%, 20%, or 30% as a result of a concurrent downward redistribution of moisture. Temperature is held constant for these results. The radiative effect of an increase of X% in column precipitable water is largely offset by a concurrent decrease of X% in the precipitable water above 600 hPa. Each reduction in the original water vapor amount above 600 hPa by 10% by redistributing it downward results in a 0.923% increase in precipitable water below 600 hPa for the TRO profile. Thus, for example, a 30% increase in total precipitable water with a 30% reduction in precipitable water between 600–200 hPa results in an increase in precipitable water below 600 hPa of 35.54%.

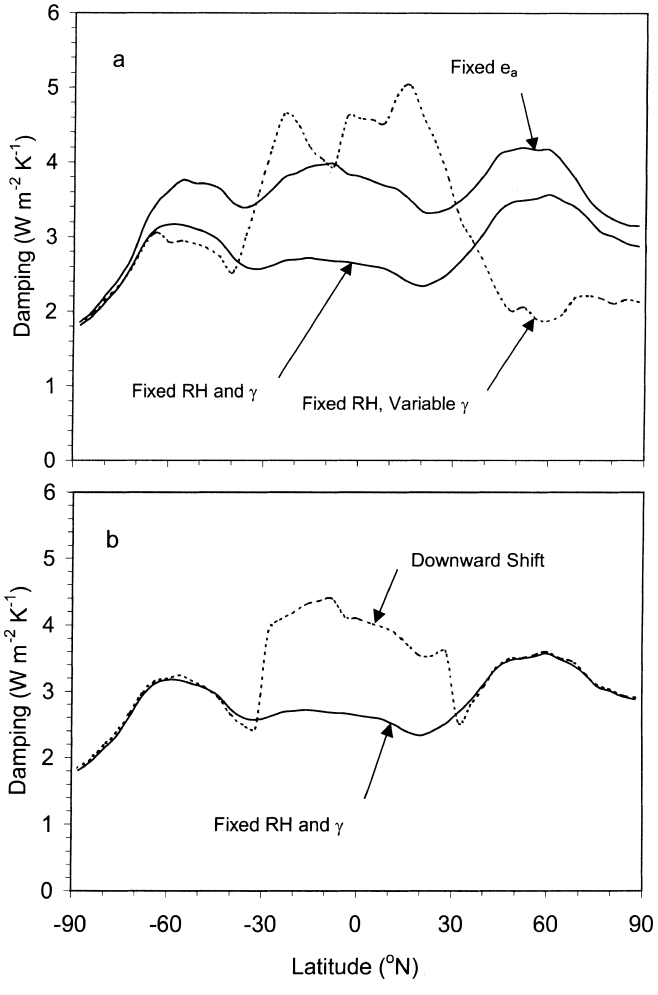

Fig. 2a, b Latitudinal variation of dF/dT_s for selected assumptions concerning changes in atmospheric humidity, lapse rate, and cloud top temperature. In **a** there is no downward shift of tropospheric water vapor, whereas **b** compares cases with fixed RH or a downward shift in water vapor using $\alpha_3 = -0.1$, assuming fixed lapse rate

Table 3 Change in surface-troposphere heating (W m^{-2}) for the McClatchey tropical profile when total precipitable water vapor is increased by X = 10%, 20%, or 30% when precipitable water between 600–200 hPa also increases by X, is held constant, or decreases by 10%, 20%, or 30% due to a downward redistribution

Column change, X	Change between 600–200 hPa				
	+X%	+0%	−10%	−20%	−30%
+10%	1.510	0.824	0.087	−0.712	−1.590
+20%	2.937	1.613	0.880	0.084	−0.791
+30%	4.289	2.367	1.636	0.843	0.030

4.2 Climate model response

The foregoing discussion of infrared flux sensitivity provides a powerful tool in understanding the climatic response to a doubling of atmospheric CO_2 with various feedback combinations in effect. The right hand portion of Table 2 shows the globally and annually averaged, steady state surface air temperature response to a CO_2 doubling, while Fig. 3 shows the latitudinal variation of mean annual, zonally averaged surface air temperature response for selected cases. The global mean temperature response obtained by the climate model is almost exactly given by the adjusted global mean radiative forcing (3.45 W m^{-2}) divided by the global mean radiative damping values given in Table 2. Also given in Table 2 are the minimum mean annual warming at any given latitude (which occurs in the tropics) and the amplification of the mean annual response from the equatorial region to polar regions.

The global mean warming with fixed RH and lapse rate is 1.50 K. The global mean warmings are 1.00 K and 1.26 K when RH is fixed everywhere or outside the 30°S–30°N region, respectively. Thus, extra-tropical water vapor feedback is responsible for about half of the total feedback for the fixed-RH case. Parametrization of the lapse rate with fixed RH reduces the tropical warming by about 25% (Fig. 3) due to the fact that γ_m (which governs the low-latitude lapse rate) decreases as the climate warms, and this serves as a negative feedback. The reduced tropical warming would also reduce

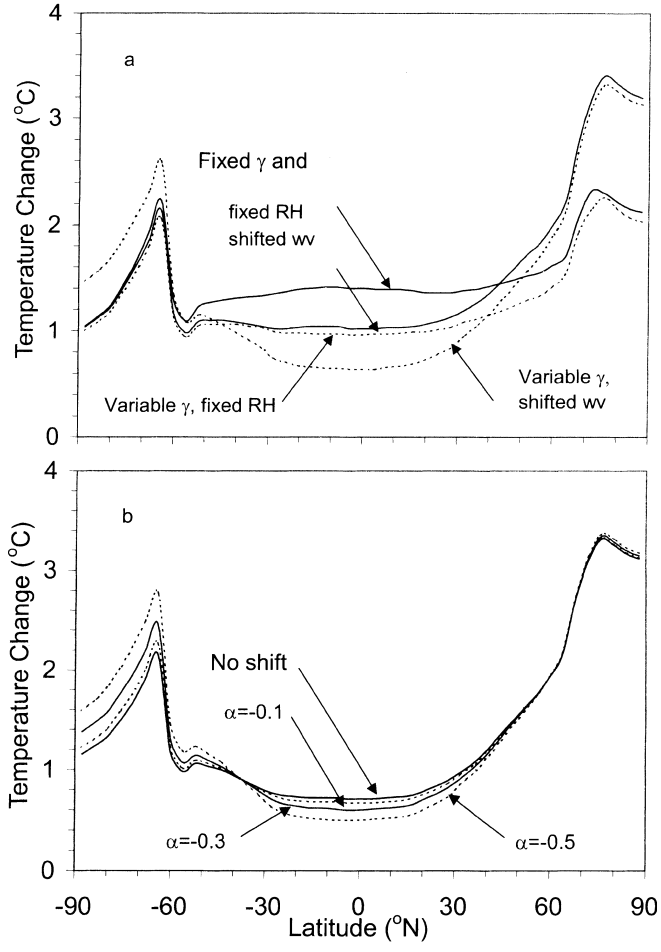

Fig. 3a, b Latitudinal variation of steady state, zonally averaged, mean annual surface air temperature change following a CO_2 doubling for **a** various assumption concerning the change in atmospheric water vapor and in tropospheric lapse rate (γ), with and without a downward shift in tropical water vapor using $\alpha = -0$; and **b** for downward shift in water vapor and for an increasingly stronger downward shift

the polar warming, but this is largely offset by the fact that γ_c (which governs the high-latitude lapse rate) increases as the meridional temperature gradient increases, and this serves as a positive feedback. The sense of the lapse rate changes obtained here is the same as obtained in the GFDL GCM (Ramanathan 1977). A decrease (increase) in the lapse rate causes upper tropospheric temperatures to be warmer (colder) than if the lapse rate is constant, which increases (decreases) infrared emission to space and thereby limits (enhances) the surface warming. The global mean response decreases by about 15%, to 1.28 K, when the lapse rate is parametrized.

When the water vapor is redistributed downward in the 30°S–30°N region using $\alpha_3 = -0.1$, the global mean surface air warming is reduced by about 15% and the tropical warming by about 30%. The strong reduction in low-latitude warming when water vapor is shifted downward at low latitudes causes a greater decrease in the middle latitude meridional temperature gradient and increase in γ_c than when RH is fixed. Since this leads to a greater increase in the middle-to-high latitude lapse rate, which serves as a positive feedback, the high-latitude response is significantly larger in spite of the reduced meridional heat transport that results from a cooler tropics (Fig. 3). Although the quantitative results shown in Fig. 3 undoubtedly depend on the way in which meridional heat transport is parametrized, these results nevertheless provide a qualitatively useful lesson: namely, the damping effect on the high-latitude warming of a strongly negative feedback operating at low latitudes can be offset to a significant extent by the increase in mid-latitude lapse rate that baroclinic instability theory suggests would occur. It is even possible that high-latitude warming increases as low latitude warming decreases.

The case with $\alpha_3 = -0.1$ can be regarded as a realistic upper limit for the strength of the surface temperature-water vapor profile feedback, based on Sinha and Allen's (1994) results. Nevertheless, as a further test of the potential for a downward shift in atmospheric water vapor to decrease climate sensitivity, a series of experiments was performed in which α_3 ranges from 0.0 K^{-1} to -0.5 K^{-1}. Global mean temperature changes are given as the last set of results shown in Table 3, while the latitudinal variation in temperature response is shown in Fig. 3b. A stronger surface temperature-water vapor distribution feedback has a rapidly diminishing marginal effect on the global mean and tropical temperature response, but causes a slight increase in high-latitude response due to the fact that the meridional temperature gradient decreases as tropical warming is reduced, which, as previously noted, leads to a larger high-latitude lapse rate. Even for the extreme and implausible case of $\alpha_3 = -0.5\,K^{-1}$, the global mean warming is about 1.0 K and high-latitude warming exceeds 3.0 K. The decreasing marginal effect on tropical temperature response is attributable to the fact that as α_3 increases, a given ΔT_s leads to a stronger downward movement of water vapor, which limits subsequent warming and hence limits the downward water vapor redistribution. Thus, as α_s varies from -0.1 to -0.3 to -0.5, the realized water vapor decrease above 600 hPa at 0°N varies from 6% to 14% to 21%.

Also shown in Table 2 is the opposite case, in which RH in the upper troposphere increases by 5% of saturation per Celsius degree warming (as in del Genio 1991). Global mean warming is enhanced by 40–60% compared to the fixed RH case, depending on whether or not the laspe rate is allowed to vary.

Finally, although the negative water vapor feedback investigated here cannot reduce the global mean climate sensitivity noticeably below 1.0 K in the present model, the tropical response is reduced by about one third for $\alpha_3 = 0.0\,K^{-1}$ (an entirely plausible value) and the equator-to-pole amplification in the zonal mean temperature response increase from about 2.0 (no downward shift in water vapor) to about 3.0 (with $\alpha_3 = 0.0\,K^{-1}$). Paleoclimatic data indicate a substan-

tially greater equator-to-pole amplification in surface temperature sensitivity than given by the current generation of coupled atmosphere-ocean general circulation models (see Hoffert and Covey 1992), although the reconstructed temperature changes remain quite uncertain. If current GCMs do indeed modestly overpredict the increase in upper troposphere water vapor at low latitudes, this could partly explain the apparent discrepancy between GCM results and paleoclimatic data. The interaction between the low-latitude water vapor feedback and the middle-to-high latitude lapse rate feedback, identified, might further contribute to the high polar amplification infered from paleoclimatic data.

5 Conclusions

This study has examined the quantitative effect on climate sensitivity of various hypothetical relationships between surface temperature and the amount and vertical distribution of water vapor in the atmosphere, with and without variable temperature lapse rates. The motivation for this study is the claim of Lindzen (1990) that enhanced cumulus convection in a warmer world will lead to drying of the upper troposphere and exert a strong negative feedback on surface temperature warming. For this purpose, an energy balance climate model with explicit infrared radiative transfer based on the NCAR CCM2 code has been used, along with parametrized temperature and RH profiles. Based on recent observational and theoretical analysis, we adopt as a likely upper limit to Lindzen's hypothesized drying a feedback such that a 1 K surface warming induces a 10% decrease in water vapor above 600 hPa, with a compensating increase below 600 hPa. Since total column precipitable water increases sharply as the surface warms, we apply this downward redistribution to a case which would otherwise entail either fixed RH or in which total precipitable water is scaled by the increase in ocean surface vapor pressure.

The key conclusions resulting from this analysis are:

1. A modest drying effect due to increased convection at low latitudes, such that absolute humidity above 600 hPa at latitudes 30°S–30°N is constant as climate warms, while total column precipitable water increases by the same amount as if relative humidity were constant, reduces the global mean temperature response by about 15% compared to the fixed relative humidity case.
2. Implementation of a progressively stronger drying feedback has a rapidly diminishing marginal effect on global mean and tropical temperature sensitivity to a CO_2 increase.
3. The suppression of tropical warming can substantially increase the polar amplification of the surface temperature response. This may have the effect of increasing the mid-to-high latitude lapse rate, which would serve as a positive feedback. In the model used here, this is sufficient to cause slightly greater polar warming as the tropical response is reduced, in spite of the fact that smaller tropical warming implies a reduced meridional heat transport.
4. Even a modest drying effect due to subsidence in the subtropical upper troposphere (i.e., sufficient to hold absolute humidity about above the 600 hPa level constant as climate warms) can reduce the tropical temperature sensitivity by one third and significantly increase the equator to pole amplification of the surface air temperature response.

By applying the hypothetical downward shift in the water vapor distribution to the entire region between 30°S and 30°N, I have probably maximized the effect on global mean climate sensitivity. If the drying mechanism were to occur in only part of the 30°S–30°N belt, for example, in the descending branches of the Hadley cells, then the reduction in global mean climate sensitivity would be smaller than obtained here. Soden (1997) showed that, as tropical Pacific sea surface temperatures increased from early 1985 to late 1988 in conjunction with an El Niño, the greenhouse trapping of infrared radiation increased between about 10°S–10°N but decreased in the descending portions of the Hadley cells. A decrease in greenhouse trapping in spite of increasing surface temperature requires at least a partial drying of the troposphere. This in turn could be due to the fact that, during an El Niño, the Hadley cell increases in strength (Pan and Oort 1983), which would tend to increase the drying tendency in the descending branches. However, the El Niño might not be an appropriate surrogate for long-term climatic change.

Ideally, one would like to compute all of the feedbacks considered here in a fully internally consistent manner as a result of specific assumptions within atmospheric GCMs. However, the sensitivity analyses presented here indicate that, whatever changes in future GCM response might occur as a result of new parametrizations of subgrid-scale processes, they are exceedingly unlikely to produce a climate sensitivity to a CO_2 doubling of less than 1 K even if the water vapor distribution changes as originally hypothesized by Lindzen (1990). This is because, although Lindzen's (1990) hypothesized drying effect can reduce global mean climate sensitivity and strongly damp the tropical temperature response, the climate sensitivity to a CO_2 doubling using a plausible upper limit to the strength of the surface temperature-upper troposphere moisture relationship is still well in excess of 1 K in the absence of cloud feedbacks. Inasmuch as observational evidence indicates that absolute humidity increases throughout the troposphere as climate warms, this casts further doubt on claims that water vapor serves as a negative feedback on the climatic response to a CO_2 increase.

Acknowledgement This research was supported by NSERC Grant OPG0001413.

References

Chylek P, Kiehl JT (1981) Sensitivities of radiative-convective models. J Atmos Sci 38: 1105–1110

del Genio A, Lacis AA, Ruedy RA (1991) Simulations of the effect of a warmer climate on atmospheric humidity. Nature 351: 382–385

del Genio AD, Kovari W, Yao MS (1994) Climatic implications of the seasonal variation of upper tropospheric water vapor. Geophys Res Lett 21: 2701–2704

Gaffen DJ, Elliot WP, Robock A (1992) Relationship between tropospheric water vapor and surface temperature observed by radiosondes. Geophys Res Let 19: 1839–1842

Hansen J, Lacis A, Rind D, Russell G, Stone P, Fung I (1984) Climate sensitivity: analysis of feedback mechanisms. In: Hansen JE, Takahashi T (eds) Climate processes and climate sensitivity, Geophys Monogr, Vol 29. AGU, Washington, pp 130–164

Harvey LDD (1988a) A semi-analytic energy balance climate model with explicit sea ice and snow physics. J Clim 1: 1065–1085

Harvey LDD (1988b) Development of a sea ice model for use in zonally averaged energy balance climate models. J Clim 2: 1221–1238

Harvey LDD (2000) Global warming: the hard science. Prentice Hall, Harlow (UK), 336 p

Hoffert MI, Covey C (1992) Deriving global climate sensitivity from palaeoclimate reconstructions. Nature 360: 573–576

Hummel JR, Kuhn WR (1981) Comparison of radiative-convective models with constant and pressure-dependent lapse rates. Tellus 33: 254–261

Kiehl JT, Briegleb BP (1991) A new parametrization of the absorptance due to the 15 um band system of carbon dioxide. J Geophys Res 96: 9013–9019

Inamdar AK, Ramanathan V (1994) Physics of greenhouse effect and convection in warm oceans. J Clim 7: 715–731

Lacis A, Hansen J (1974) A parametrization for the absorption of solar radiation in the Earth's atmosphere. J Atmos Sci 31: 118–139

Lindzen R (1990) Some coolness concerning global warming. Bull Am Meteorol Soc 71: 288–299

Manabe S, Wetherald RT (1967) Thermal equilibrium of the atmosphere with a given distribution of relative humidity. J Atmos Sci 24: 241–259

Manabe S, Wetherald RT (1980) On the distribution of climate change resulting from an increase in CO_2 content of the atmosphere. J Atmos Sci 37: 99–118

Mackay RM, Khalil MAK (1991) Theory and development of a one dimensional time dependent radiative convective climate model. Chemosphere 22: 383–417

McClatchey RA, Fenn RW, Selby JEA, Volz FE, Garing JS (1971) Optical properties of the atmosphere. Rep AFCRL-71-0279, 85 pp, Air Force Cambridge Res Lab, Cambridge, Mass

Mitchell JFB, Ingram WJ (1992) Carbon dioxide and climate: mechanisms of changes in cloud. J Clim 5: 5–21

Mokhov II, Schlesinger ME (1994) Analysis of global cloudiness 2. Comparison of ground-based and satellite-based cloud climatologies. J Geophys Res 99: 17 045–17 065

Ramanathan V (1977) Interactions between ice-albedo, lapse-rate and cloud-top feedbacks: An analysis of the nonlinear response of a GCM climate model. J Atmos Sci 34: 1885–1897

Ramanathan V, Coakley JA (1978) Climate modeling through radiative convective models. Rev Geophys Space Phys 16: 465–489

Ramanathan V, Dickinson R (1979) The role of stratospheric ozone in the zonal and seasonal radiative energy balance of the earth-troposphere system. J Atmos Sci 36: 1084–1104

Ramanathan V, Downey P (1986) A nonisothermal emissivity and absorptivity formulation for water vapor. J Geophys Res 91: 8649–8666

Rind D, Chiou EW, Chu W, Larsen J, Oltmans S, Lerner J, McCormick MP, McMaster L (1991) Positive water vapour feedback in climate models confirmed by satellite data. Nature 349: 500–503

Shine KP, Sinha A (1991) Sensitivity of the Earth's climate to height-dependent changes in the water vapour mixing ratio. Nature 354: 382–384

Sinha A, Allen MR (1994) Climate sensitivity and tropical moisture distribution. J Geophys Res 99: 3707–3716

Soden BJ (1997) Variations in the tropical greenhouse effect during El Niño. J Clim 10: 1050–1055

Spelman MJ, Manabe S (1984) Influence of oceanic heat transport upon the sensitivity of a model climate. J Geophys Res 89: 571–586

Stone PH, Carlson JH (1979) Atmospheric lapse rate regimes and their parametrization. J Atmos Sci 36: 415–423

Sun DZ, Lindzen RS (1993) Distribution of tropical tropospheric water vapor. J Atmos Sci 50: 1643–1660

Sun DZ, Oort AH (1995) Humidity-temperature relationships in the tropical troposphere. J Clim 8: 1974–1987

Thompson SL, Warren SG (1982) Parametrization of outgoing infrared radiation derived from detailed radiation calculations. J Atmos Sci 39: 2667–2680

Wetherald RT, Manabe S (1975) The effects of changing the solar constant on the climate of a general circulation model. J Atmos Sci 32: 2044–2059

Zhang MH, Hack JJ, Kiehl JT, Cess RD (1994) Diagnostic study of climate feedback processes in atmospheric general circulation models. J Geophys Res 99: 5525–5537